

NANO | MICRO

small

Plasmonic Coupling

A reproducible high-throughput approach is reported by J. J. Li, C. Z. Gu, and co-workers on page 3933 to fabricate wafer-scale double-layer stacked Au/ Al_2O_3 @Au(Ag) nanosphere structures with tunable nanospacing for surface-enhanced Raman scattering. This nanostructure constitutes a 3D plasmonic nanostructure with tunable nanospacing and high-density nanojunctions between adjacent Au nanospheres of ultrathin Al_2O_3 isolation layers, producing highly strong plasmonic coupling so that the electromagnetic near-field is greatly enhanced to obtain a uniform increase of SERS with an enhancement factor of over 108.

19/2014

WILEY-VCH

Wafer-Scale Double-Layer Stacked Au/ Al_2O_3 @Au Nanosphere Structure with Tunable Nanospacing for Surface-Enhanced Raman Scattering
J. J. Li, C. Z. Gu, and co-workers

Wafer-Scale Double-Layer Stacked Au/ Al_2O_3 @Au Nanosphere Structure with Tunable Nanospacing for Surface-Enhanced Raman Scattering

Zhaosheng Hu, Zhe Liu, Lin Li, Baogang Quan, Yunlong Li, Junjie Li,* and Changzhi Gu*

Fabricating perfect plasmonic nanostructures has been a major challenge in surface enhanced Raman scattering (SERS) research. Here, a double-layer stacked Au/ Al_2O_3 @Au nanosphere structures is designed on the silicon wafer to bring high density, high intensity “hot spots” effect. A simply reproducible high-throughput approach is shown to fabricate feasibly this plasmonic nanostructures by rapid thermal annealing (RTA) and atomic layer deposition process (ALD). The double-layer stacked Au nanospheres construct a three-dimensional plasmonic nanostructure with tunable nanospacing and high-density nanojunctions between adjacent Au nanospheres by ultrathin Al_2O_3 isolation layer, producing highly strong plasmonic coupling so that the electromagnetic near-field is greatly enhanced to obtain a highly uniform increase of SERS with an enhancement factor (EF) of over 10^7 . Both heterogeneous nanosphere group (Au/ Al_2O_3 @Ag) and pyramid-shaped arrays structure substrate can help to increase the SERS signals further, with a EF of nearly 10^9 . These wafer-scale, high density homo/hetero-metal-nanosphere arrays with tunable nanojunction between adjacent shell-isolated nanospheres have significant implications for ultrasensitive Raman detection, molecular electronics, and nanophotonics.

1. Introduction

Plasmonic couplings between adjacent noble metal nanoparticles have been extensively investigated both experimentally and theoretically, with the finding that they can produce strong electromagnetic focusing effect with a concomitant local field enhancement, and hence are favorable for a large increase of optical response.^[1–6] This opens a route to numerous practical applications, such as optical nanoantennas, surface enhanced Raman scattering (SERS) or fluorescence of molecules or to create high-sensitivity sensors.^[7–9] Particularly, SERS is widely used to identify the

chemical fingerprints by taking full advantage of the strong enhancement of local field induced by plasmonic coupling, called electromagnetic “hot spots.” Fabricating perfect plasmonic nanostructures based on metallic nanoparticle for high density, high intensity “hot spots” has been a major challenge in SERS research. Precisely tunable position of adjacent metal nanoparticles is a key factor to bring about intense plasmonic coupling; however, controlled fabrication is still a great challenge.

So far, numerous efforts have been made to design diverse forms of noble metallic nanoparticle as SERS substrates, in which metallic nanoparticles in colloidal solution is broadly adopted to form SERS substrate, showing a large enhancement factors and even a great potential in single molecule detection.^[10–12] However, with colloidal solution it is a challenge to control position of adjacent metal nanoparticles and bring the metal nanoparticle sufficiently close to form hot spots around the analyte, while at the same time preventing the formation of large conglomerations of nanoparticles before the analyte is introduced. Although improved results based on self-assembled colloidal nanoparticles are recently reported to form sub-10 nm gaps between nanoparticles

Z. S. Hu, Z. Liu, L. Li, Dr. B. G. Quan, Dr. Y. L. Li,
Prof. J. J. Li, Prof. C. Z. Gu
Beijing National Laboratory for
Condensed Matter Physics
Institute of Physics
Chinese Academy of Sciences
Beijing 100190, P. R. China
E-mail: jjli@iphy.ac.cn; czgu@iphy.ac.cn
DOI: 10.1002/smll.201400509



tuned by using CTAB, and it still is very difficult for colloidal suspensions of metallic nanoparticle to control in the process of wafer-scale, clean background and uniform fabrication. A perfect SERS substrate would have not only reproducible and large Raman enhancement over wide areas, but also can ideally be fabricated by an inexpensive and high-throughput method.

Metallic nanoparticles can also be prepared by combining metal film's physical deposition with annealing treatment process, but it is still difficult to reduce the distance between metal nanoparticles to nanoscale for originating nanojunctions over a large area by present nanotechnology.^[13,14] The nanospacing or nanojunction between adjacent metal nanoparticles is responsible for nearest-neighbor plasmonic coupling, which can produce strong "hot spots," according to theoretical and experimental reports,^[2–6] and the "hot spots" contribute greatly to overall SERS signals. Thus it is highly desirable to control the position and density of these "hot spots" by tuning nanospacing or nanojunction between adjacent metal nanoparticles in a large-area substrate.

Here we present a far simple method of controlling the position of adjacent metal nanoparticles, producing large-area sub-5 nm nanospacing with high-density nanojunctions between adjacent metal nanoparticles by constructing double-layer Au/Al₂O₃@Au nanosphere stacked structure. In order to control the position of metallic nanosphere and form nanospacing with nanojunction between nanospheres, Al₂O₃ ultrathin film is coated on one metal nanosphere to isolate nanosphere from another metal nanosphere, and thus the nanospacing and nanojunction can be precisely tuned by the thickness of Al₂O₃ film. This approach—with no high-end nanofabrication techniques—is an easily reproducible, high-throughput way to form sub-5 nm nanospacing and hence dense nanojunctions for high intensity hot spots effect. This method has some outstanding advantages, such as wafer-scale, uniform, easily patterned fabrication, precisely controllable nanospacing and the option of adjacent homo-nanospheres or hetero-nanospheres. Another advantage of this structure is that it may have a clean background, which is very important for further applications. On the other hand, the as-fabricated double-layer stacked metal nanosphere array are able to construct a complex 3D nanoplasmonic network-structure with controlled nanospacing and high-density nanojunctions, which contribute remarkably large Raman enhancement due to highly intense "hot-spots" effect induced by greatly enhanced electromagnetic near-field between neighboring metal nanospheres. This tuned nanospacing inducing high-density nanojunctions between adjacent shell-isolated metal nanospheres, when made possible on a large scale, has significant implications for ultrasensitive Raman detectors, molecular electronics and nanophotonics.

2. Results and Discussions

2.1. FDTD Simulation of Adjacent Metallic Nanospheres

Figure 1 shows the Finite-difference time-domain (FDTD) simulation results of the distribution of "hot spots" and

localized electric field in different positions of adjacent Au nanospheres with 30 nm size. We can see that the case of contacted nanospheres and 3 nm nanogap structure only has a single "hot spots" region (Figure 1a,b) while 3 nm nanospacing produced by a 3 nm thick dielectric layer in Au/Al₂O₃@Au nanosphere structure has two "hot spots" regions: dielectric nanospacing region (Al₂O₃ layer) and nanojunction region outside dielectric layer (Figure 1c,c') corresponding to different "hot spots" intensities, but only the nanojunction region is an effective region for SERS detection because the analytes can get into this region while Al₂O₃ layers would block analytes from entering the dielectric nanospacing region though it has a strong "hot-spots" effect. Figure 1e shows FDTD simulation results of the near-field enhancement factor $|E/E_0|$ at different positions and regions of nanosphere dimer, indicating that the nanojunction outside of 3 nm Al₂O₃ layer nanospacing exhibits "hot spots" similar in intensity to those in 3 nm nanogap structure, certified by calculation results that the $|E/E_0|$ in the region of 3 nm nanogap and local junction region of nanosphere dimer with Al₂O₃ layer nanospacing is estimated to be about 16.3 and 16.7, respectively. Further, the dielectric region of nanosphere dimer shows a distinct enhancement of localized electric field ($|E/E_0| = 25.4$), and thus a stronger electric field in dielectric region also will increase the "hot spots" intensity in adjacent nanojunction region. When Au nanosphere isolated by Al₂O₃ layer is replaced to Ag nanosphere, Au/Al₂O₃@Ag hetero-dimer structure exhibits a stronger "hot spots" than the former homo-dimmers. In the case of model systems formed by interacting Au and Ag nanosphere, there are two resonances with wavelengths close to those of localized surface plasmon resonance of isolated Au and Ag nanosphere.^[15,16] Their electromagnetic coupling leads to a large enhancement of optical response. For this Au/Al₂O₃@Ag hetero-dimer structure, their near-field enhancement factor $|E/E_0|$ of dielectric spacing region (Figure 1d) and nanojunction region (Figure 1d') is estimated to be about 47.8 and 30.9, respectively. It can be seen that for adjacent Au nanospheres isolated by Al₂O₃ layer, the nanojunction region outside of the dielectric region have also rather strong electromagnetic field distribution, which is important to enhance the Raman signal. Above results of FDTD simulation testified the feasibility of our strategies of constructing double-layer stacked Au/Al₂O₃@Au nanosphere structure for SERS.

2.2. Fabrication Process and Characterization

Figure 2 shows a schematic of the fabrication process of plasmonic nanostructure of Au nanosphere using a two RTA steps with an intervening ALD process. First, Au nanosphere arrays are prepared by RTA of a 2–7 nm thick Au nanofilm deposited on the silicon wafer using e-beam evaporation, as showed in Figure 2a,b. Then, a sub-5 nm Al₂O₃ layer is uniformly deposited on one of the Au nanosphere arrays via an ALD process, resulting in excellent surface coating, as shown in Figure 2c. Next, another 2–7 nm thick Au film was deposited on the shell-coated nanosphere arrays, and subsequent second RTA process is again carried out to form another

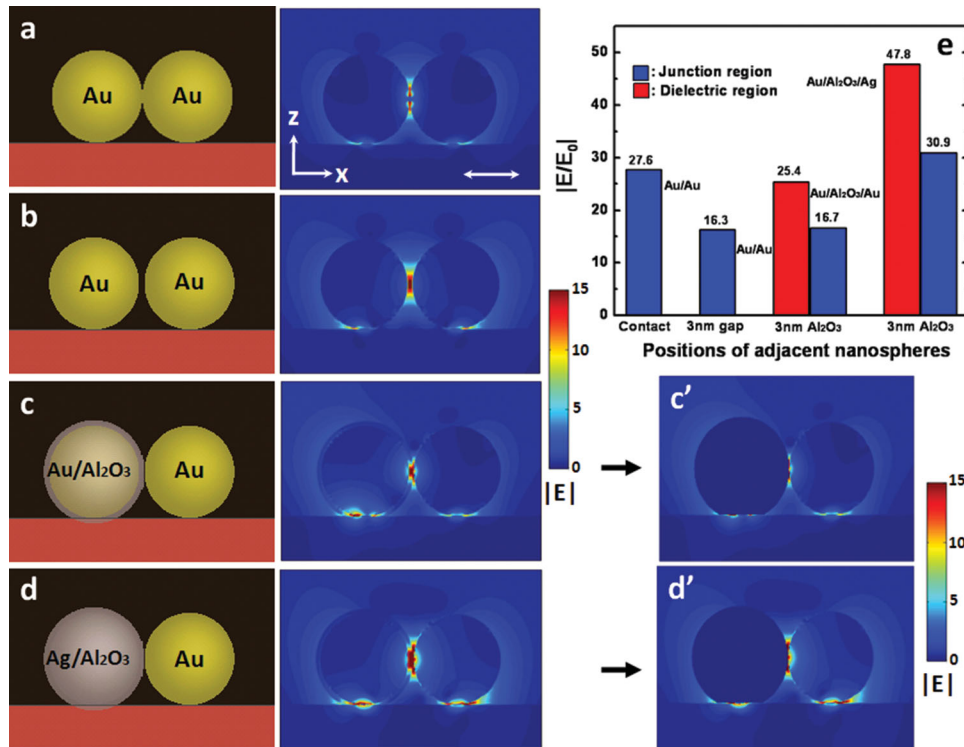


Figure 1. FDTD simulations showing the x - z view of electromagnetic field distribution of different positions and regions of adjacent metallic nanospheres with 30 nm in size. a) contacted and b) 3 nm nanogap of Au nanosphere dimer. 3 nm thick Al_2O_3 spacing isolating c) $\text{Au}/\text{Al}_2\text{O}_3@\text{Au}$ nanosphere and d) $\text{Au}/\text{Al}_2\text{O}_3@\text{Ag}$ nanosphere. c',d') Real nanojunction region outside of Al_2O_3 layer between adjacent nanospheres, based on (c,d) after shielding this Al_2O_3 dielectric spacing region. e) The histogram of a near-field enhancement factor $|E/E_0|$ at different positions and regions of nanosphere dimer structure. The incident light wavelength is 600 nm. The white arrow indicates the polarization direction of the incident light.

Au nanosphere arrays on the original Au nanosphere arrays isolated by Al_2O_3 layer (Figure 2d,e). Even double-layer or multi-layer stacked Au nanosphere structures can be fabricated successfully by repeating the above process. In the whole process, the coordination of the RTA and ALD processes is very critical, since the RTA process can control the size of the Au nanospheres while the ALD process can tune the nanospacing between nanospheres by coating thin Al_2O_3 layer with angstrom-scale thickness resolution, uniformity, as well as nearly perfect conformality. It is particularly important that the Al_2O_3 layer has a very high melting point to protect the original Au nanosphere arrays during second RTA. It is noteworthy that due to the influence of gravity during the RTA process and the interaction between the two layers following the principle of minimum energy, two Au nanosphere layers are closely stacked. Figure 2f,g is a model showing that a minimum unit of double-layer stacked Au nanospheres is similar to a like-tetramer structure, including three local nanojunction regions outside of nanospacing. A well-formed nanojunction-rich three-dimension structure can include a high density of sites for localization of electromagnetic field and thus highly sensitive detection sites for SERS.

In the above scheme, the nanospacing is determined by the thickness of the Al_2O_3 layer, which can be precisely controlled by the number of ALD cycles. Furthermore, because these stacked Au nanosphere arrays are made via a wafer-scale batch process, high density nanospacing and nanojunction can be readily fabricated over a 4 inch wafer, which is

very difficult to accomplish by chemical self-assembly and the usual lithography technology. **Figure 3a–c** show the scanning electron micrograph (SEM) images from 4 nm thick Au film to single-layer Au nanosphere and double-layer stacked Au nanosphere ($\text{Au}/\text{Al}_2\text{O}_3@\text{Au}$). This process at 450 °C RTA transforms 4 nm thick Au film into uniform Au nanosphere arrays with average size and spacing of 30 nm, and then 3 nm thick Al_2O_3 film is deposited by ALD. After another deposition of Au nanofilm and second RTA process, double-layer stacked structure of Au-nanospheres/ $\text{Al}_2\text{O}_3@\text{Au}$ -nanospheres is formed. In order to clearly observe the double-layer nanosphere structure, a high-resluoion SEM of the local area is displayed in the Figure 3d. We can discern the formation of double-layer stacked Au nanosphere structure with dense like-tetramer constitutional unit marked by arrows, in which the darker regions at the center of most of the areas identified by the arrows are bottom Au particles coated by Al_2O_3 layer. Particularly, the transmission electron microscope (TEM) image of a single Au nanosphere coated by Al_2O_3 layer is give in Figure 3e, indicating the thickness of Al_2O_3 isolated shell is in the range of 3–5 nm. Figure 3f shows a 4 inch wafre-scale smaple of double-layer stacked Au nanospheres, verifing a large-scale and high thoughput nano-fabricating ability as SERS substrate. In addition, the shape, size and spacing of Au nanospheres are also key factors, because they can influence the distribution of local surface charge among the neighbor nanospheres and hence change the plasmon resonance. In addition, anneal time should be

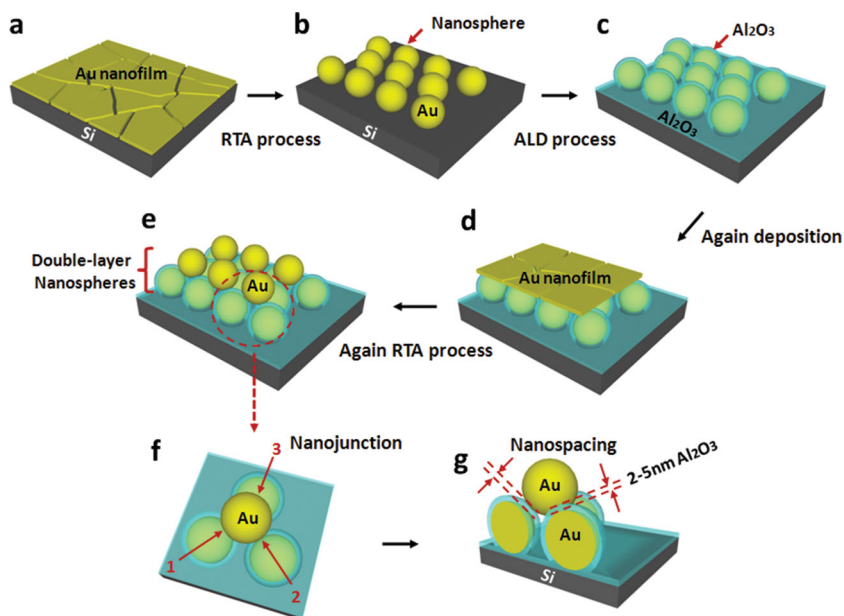


Figure 2. Schematic of fabrication process for high density plasmonic nanospacing and nanojunction between adjacent Au nanospheres. a) A thin Au film deposited by E-beam evaporation on the silicon wafer and b) Au nanosphere arrays produced by RTA process. c) ALD process coats thin Al_2O_3 layer on the surface of Au nanospheres. d,e) Another thin Au film deposit on the $\text{Al}_2\text{O}_3/\text{Au}$ nanosphere, followed by RTA process to form a stacked structure of Au nanospheres/ $\text{Al}_2\text{O}_3@\text{Au}$ nanospheres with nanospacing. f,g) Platform and section of a minimum unit of double-layer stacked Au nanosphere, similar to tetramer structure including three nanospacings and nanojunctions, which can cause the formation of which can cause the formation of nanojunction-rich network structure in the three-dimension spacing when the large-scale sample is fabricated.

controlled during RTA process, attributing to lower surface energy of bigger sphere, the long annealing time can make the bigger sphere become bigger and the smaller become smaller while the short time cannot change a Au nanoisland to a nanosphere. Figure 3g gives the dependence of average size and density of Au nanosphere on the Au film thickness under 450 °C RTA process for 3 mins. The results show that an increase of film thickness from 2 nm to 8 nm can reduce the array-density of the Au nanospheres, but increase the average size of the Au nanospheres. Therefore, in addition of ALD process, both a suitable Au film thickness and optimized annealing process are required to form uniform double-layer stacked Au nanosphere arrays because the uniformity of as-formed Au nanosphere is an important aspect of a compelling SERS substrate. Due to the nonperiodic nanostructure for our sample, the uniformity of the substrate structure can be estimated by the uniformity of the distribution density of metal nanosphere in the substrate, including two key factors: average nanosphere size and interparticle spacing, which can be tuned by accurately controlling the thickness of Au film, temperature and duration of RTA. In this work, a distribution density of Au nanosphere of $\approx 10^3/\mu\text{m}^2$ with an average size of ≈ 30 nm and average spacing ≈ 30 nm can be selected as the sample for SERS measurement, which can be estimated by statistical count based on high-resolution SEM image such as Figure 3b, and also this nanoparticle size have been reported to be favorable for increasing Raman signal.^[17,18] For an area of 1 cm \times 1 cm in such substrate, the uniformity

of Au nanosphere density (about $10^3/\mu\text{m}^2$) is confirmed to be $\approx 5\%$ by multiple measurements at different locations.

2.3. Optical Response Performance

To characterize the optical response performance of samples fabricated at the optimal process, the reflectance spectra of single and double layer structures were measured, as shown in **Figure 4a**. It is found that the double-layer sample exhibits a more intense resonance peak at ≈ 600 nm than does the single-layer sample, which is attributed to the plasmonic coupling effect between the two layers and to very dense sub-5 nm spacing between adjacent Au nanospheres, resulting in electromagnetic field confinement and hence strong localized surface plasmon resonance (LSPR). Compared with individual or sparse Au nanoparticles with a resonance peak of ≈ 550 nm, a red-shift in our sample is attributed to plasmon coupling between adjacent Au nanospheres in single-layer versus double-layer structure. In addition, the sizes, shapes and aggregated states of Au nanoparticles all can cause the red-shift of the resonance peak.^[19,20]

To understand the physical mechanism behind electromagnetic field confinement in the nanospacing between adjacent Au nanospheres, FDTD calculations were used to simulate the electromagnetic field distribution excited with a laser of 600 nm. The simulation area consists of a single like-tetramer stacked 30 nm Au nanosphere with a 3 nm nanospacing Al_2O_3 layer and among nearest-neighbor two Au nanosphere between double-layers, as shown in Figures 4b,c, in which we are only concerned about the distribution of the nanojunction regions outside the Al_2O_3 dielectric region between nanospheres, shielding the dielectric region to eliminate its effects. We can see that strong field is confined within three nanojunction regions outside 3 nm dielectric nanospacing around a like-tetramer stacked structure, which can increase the areal density of “hot spots” within the detection volume compared with the dimer structures. And further, a large-area like-tetramer stacked nanosphere structure leads to the formation of the high-density nanojunctions in three-dimensional space that are very advantageous for the generation of a very dense population of hot-spots. A near-field enhancement factor $|E/E_0|$ in the nanojunction region shown in Figure 4c is estimated to be about 63.8, which is much higher than the $|E/E_0|$ results of adjacent nanospheres with different positions shown in Figure 1e, indicating evidently that the adjacent Au nanospheres in the three-dimension structure have an more intensive hot spots effect than those on the plane shown in Figure 1. Therefore, for the whole double-layer stacked Au nanosphere structure, large area nanojunction-rich can generate strongly localized

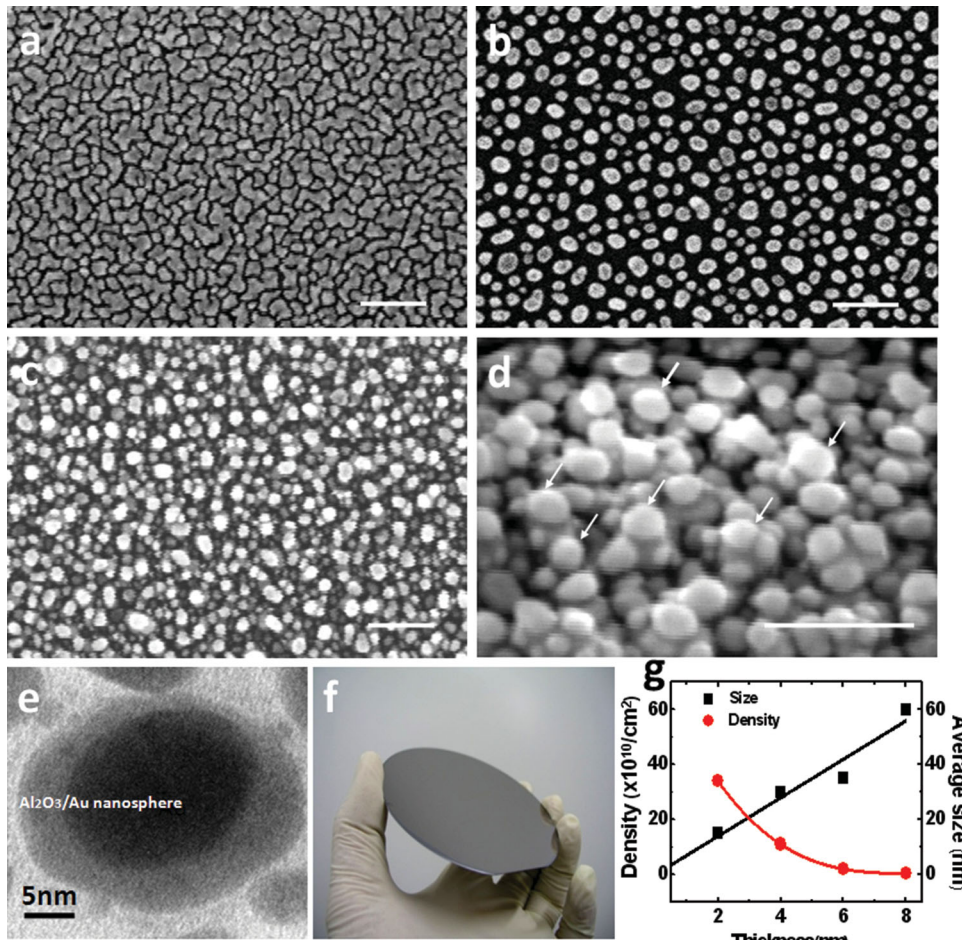


Figure 3. SEM image of 4 nm gold film a) before RTA and b) after RTA, single Au nanosphere arrays. c) Double-layer stacked Au/ Al_2O_3 /Au nanosphere structure. d) A high resolution SEM image of local area of stacked structure, verifying the formation of double-layer stacked Au nanosphere structure with dense like-tetramer constitutional unit (marked by arrows). Scale bar in SEM image, (a-d) 100 nm. e) TEM image of a single Au nanosphere coated by Al_2O_3 layer, indicating the the thickness of Al_2O_3 isolated shell is in the range of 3–5 nm. f) The 4 inch wafer sample of double stacked Au/ Al_2O_3 @Au nanosphere structure. g) Dependence of average size and density of Au nanosphere on the Au film thickness under 450 °C RTA process for 3 min.

and high-density hot spots to increase SERS enhancement factor due to its three-dimensional distribution. In addition, this like-tetramer structure has stronger and denser electromagnetic fields than nanoparticle dimers^[21,22] because of the much greater extent of the overlap of the dipoles between adjacent particles, and this dipole character ensures strong coupling to electric dipolar excitation for higher enhancement factor of SERS.

2.4. SERS Measurements

The SERS spectra of the Au nanosphere substrate were measured by a confocal Raman microscope with 532 nm excitation after introduction of analytic molecules. Differently prepared samples were used as SERS substrate, and neat self-assembled monolayer of 4-nitrobenzenethiol (4-NBT) as adsorbate molecule is coated on these samples. **Figure 5a** shows the

SERS spectra of single layer Au nanosphere and double-layer stacked Au nanosphere. According to Raman spectra, 4 main strong peaks appear at 1081 cm⁻¹ (S-C stretching vibration), 1099 cm⁻¹, 1340 cm⁻¹ (stretching vibration (NO_2)),

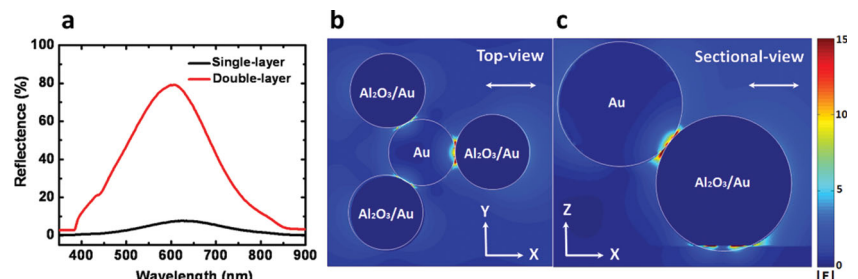


Figure 4. a) Measured reflectance spectra of single-layer Au nanosphere arrays and double-layer stacked Au nanosphere structure, average size and spacing of Au nanosphere are ≈ 30 nm, Al_2O_3 isolated-layer is 3 nm thick, b) and c) FDTD simulation showing the x-y and x-z view of electromagnetic field distribution around like-tetramer stacked structure after shielding 3 nm dielectric nanospacing that is not an effective region for SERS detection, in which the left and right gives the top view of like-tetramer and the sectional view of double-layer, respectively. It can be seen that strong fields are confined within three nanojunction regions outside dielectric layer nanospacing, contributing to large enhancement of SERS signals. The incident light wavelength is 600 nm. The white arrow indicates the polarization direction of the incident light.

1578 cm⁻¹ (C=C stretching vibration of the benzene ring) and a weaker peak 1182 cm⁻¹,^[23] in which the SERS signature peak of double-layer stacked Au nanospheres at 1340 cm⁻¹ from stretching vibration mode is clearly distinguishable, and its peak intensity is two orders of magnitude higher than that of single layer Au nanospheres. An EF of Au nanospheres sample is calculated based on the surface area of the entire Au nanosphere structure rather than the local surface area only considered at nanospacing. The double-layer stacked Au/Al₂O₃@Au nanospheres structure shows an enhancement factor of over $\sim 10^7$ that is much higher than the $\sim 10^5$ factor of single layer Au nanospheres, and this significant increase in EF contributes dominantly high dense “hot spots” induced by numerous nanojunction outside sub-5 nm nanospacings where the signals are focused to produce strong near-field plasmonic coupling. In order to further tune local plasmonic coupling of nanospacing between adjacent Au nanospheres and achieve the maximum Raman signal enhancement, the number of stacked layers, isolating layer’s thickness (Al₂O₃ layer) and presence of hetero-nanospheres are changed to observe the SERS effect. Figure 5b,c showed a change of Raman spectra with stacked layer number and Al₂O₃ isolated layer thickness, respectively. The results indicate that the increase of the layer number of stacked Au nanosphere from 2 to 4 layer reduce the SERS greatly instead of increasing Raman signal, and the sharp drop of Raman signal intensity corresponds to the histogram of Raman intensities shown

in a inset of Figure 5b. Multi-layer stacked Au nanospheres show a layer-symmetry structure, which can weaken the dipole moment and reduce the plasmonic coupling between layers.^[24] Figure 5c also shows that a 3 nm thick isolating layer is an optimal nanospacing for SERS – more than 3 nm will weaken the plasmonic coupling effect between adjacent Au nanospheres, while less than 3 nm can lead to the overlap the electronic densities of nanoparticles and even electron tunneling across the junction that reduces the coupling between two nanoparticles and field enhancement.^[25,26] And thus, the double-stacked Au nanosphere structures with 3 nm spacing is the optimal structure for very intense SERS. The above results reflect the plasmonic coupling between homogeneous metal nanospheres (Au/Al₂O₃/Au), and Figure 5d gives the effect of heterogeneous metal nanospheres (Au/Al₂O₃/Ag) on SERS. We can see that this double stacked heterogeneous metal nanosphere structure leads to a large enhancement of SERS compared to homogeneous metal nanospheres (Au/Al₂O₃/Au), and the EF are increased from $\approx 4 \times 10^7$ to $\approx 2 \times 10^8$. This large SERS enhancement comes from the combined effect of two resonances together with near field enhancement in the optical responses of heterogeneous Ag-Au nanospheres, which produces significant electromagnetic coupling between Ag and Au nanospheres that is responsible for the very intense SERS.^[27-29]

Above measured results are completely in accord with the FDTD simulation in Figure 1c,c’,d,d’, demonstrating the

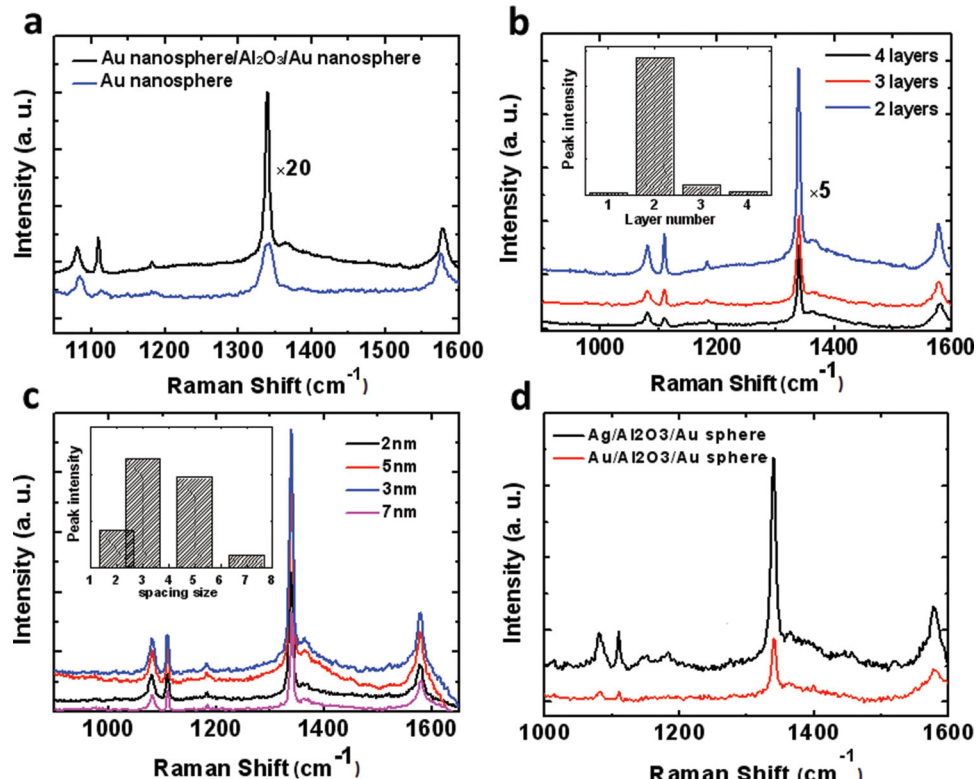


Figure 5. The SERS spectra of 4-NBT molecules measured with various substrates. a) Single and double Au nanosphere arrays. b) Au nanosphere stacked structure with different layers. c) Double-layer Au nanosphere/Al₂O₃@Au nanosphere with different Al₂O₃ thicknesses. d) Hetero-nanospheres stacked structure (Au /Al₂O₃@Ag) compared with homo-nanospheres (Au/Al₂O₃@Au) . Inseted “ $\times 20$ ” and “ $\times 5$ ” in (a,b) represent a real signal intensity should be 20 times and 5 times the level of a Raman signal shown in (a,b), and this reduced Raman signal is in order to easily compare with another peaks.

heterogeneous metal nanospheres ($\text{Au}/\text{Al}_2\text{O}_3@\text{Ag}$) structure increases greatly the electromagnetic field intensity in both the dielectric nanospacing and nanojunction region compared with homogeneous metal nanospheres ($\text{Au}/\text{Al}_2\text{O}_3@\text{Au}$). The near-field enhancement factor $|E/E_0|$ of the hetero-nanospheres structure in the junction region is estimated to be 30.9 that much higher than the $|E/E_0|$ of 16.7 for the homo-nanospheres structure, as shown in Figure 1e. Especially strong fields are confined within nanojunction region between adjacent hetero-nanospheres, but hetero-nanospheres create a larger field anisotropy with larger local enhancement due to the combined effect of electromagnetic coupling.

A large scale uniformity and repeatability of SERS signal in such substrate need to be verified further. **Figure 6a** shows a Raman map across a $1 \text{ cm} \times 1 \text{ cm}$ piece of double-layer nanosphere surface, in which the relative intensity of the 1340 cm^{-1} peak is mapped using a laser spot diameter of $1 \mu\text{m}$ and a step-size of $0.3 \mu\text{m}$. Five typical mapping areas with $2 \mu\text{m} \times 2 \mu\text{m}$ in area distributed over different locations of the sample show a good uniformity with a below 10% deviation from the average signal, in which few regions with too stronger and weaker signal have not been considered as real data to evaluate the Raman signal uniformity. Figure 6b shows a repeatability of SERS measurement for the same sample, in which five SERS measurements with 2 hour

intervals are completed, displaying a small fluctuation of Raman signal to verify a good repeatability. In addition, this Au nanosphere substrate can be used in quantitative analysis of SERS. The SERS spectra of 4-NBT solution with different concentrations have been measured on the same substrate, as showed in the Figure 6c,d. We find that the intensity of SERS signature peak is reduced gradually with decreasing the concentration, in which the SERS signature peak of 10 nm 4-NBT at 1340 cm^{-1} from stretching vibration mode is clearly distinguishable, but when the concentration is lowered to 1 nm , the SERS signature peak become very weak and almost disappearing. This quantitative analysis results indicate that double-layer stacked Au nanospheres structure has strong detecting ability by SERS signature at nanomolar level and even opens up the opportunity for SERS at single-molecule level.

In order to further increase the SERS properties of this double-layer stacked metal nanospheres structure, large-area silicon pyramid-shaped arrays are fabricated by chemical wet-etching, and then double-layer stacked metal nanospheres form on the surface of pyramid-shaped structure arrays as new SERS substrate. **Figure 7a,b** show as-fabricated silicon pyramid-shaped structure arrays with $9 \mu\text{m}$ period and a unit structure has $3 \mu\text{m}$ height and $5 \mu\text{m}$ base-line length. Figure 7c displays a top-view SEM image of single silicon pyramid-shaped structure coated

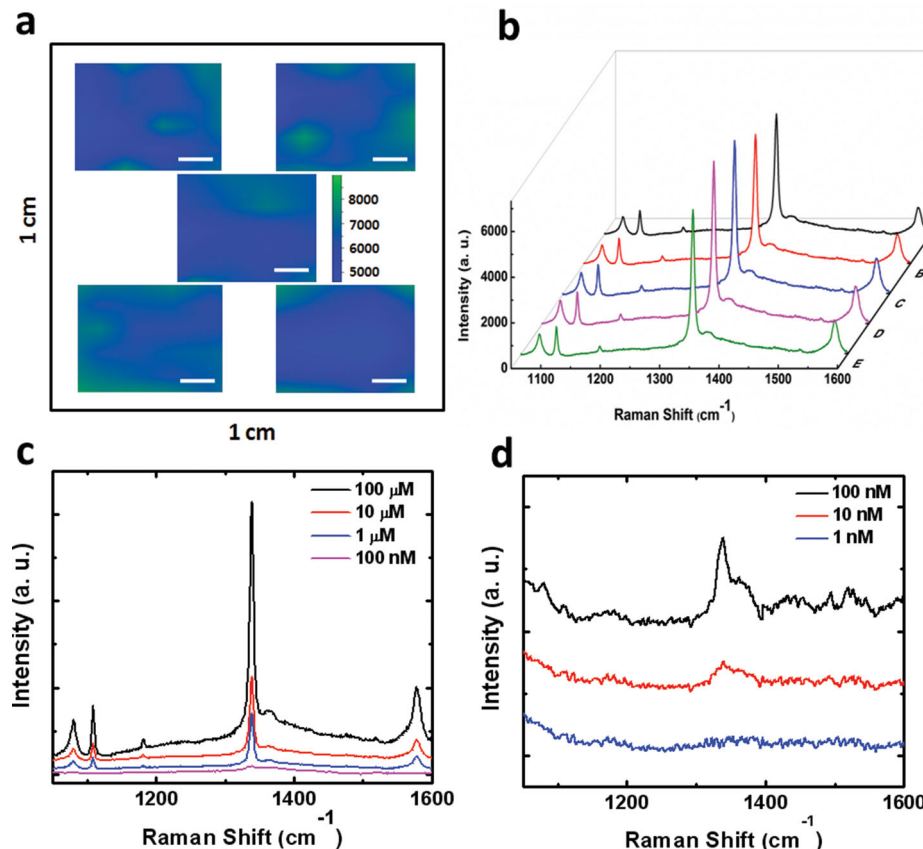


Figure 6. a) Raman Maps showing the uniformity of SERS signal across a $1 \text{ cm} \times 1 \text{ cm}$ piece of stacked nanosphere surface, and five different areas are Raman mapped and its scale bar is $0.5 \mu\text{m}$. b) Repeatability measurement of SERS signal in the same sample, including five SERS measurement processes with 2 h intervals. c,d) Change of SERS signal of 4-NBT solution with different concentrations on the same substrate. When the solution concentration is lowered to 1 nm , the SERS signature peak become very weak and almost disappearing.

by double-layer stacked metal nanospheres, reflecting distinctly the uniform distribution of metal nanospheres on the surface silicon pyramid-shaped structure. The SERS spectra of different substrates with double-layer stacked metal nanospheres are shown in Figure 7d. It can be seen that the silicon pyramid-shaped array structure shows a clear superiority in enhancing the Raman signal and surpasses the planar structure. Both homo-nanospheres ($\text{Au}/\text{Al}_2\text{O}_3@\text{Au}$) and hetero-nanospheres ($\text{Au}/\text{Al}_2\text{O}_3@\text{Ag}$) have a significant increase of SERS effect with the help of the pyramid-shaped structure, which corresponds to the EF of $\approx 2 \times 10^8$ and nearly 10^9 , respectively, and the latter has 4 times improvement in the Raman signal intensity relative to the former. The SERS spectra were measured from randomly selected 20 spots over the SERS pyramid-shaped substrate, and each measured-spot only includes a single pyramid-shaped structure. The results show an average SERS EF of near to $\sim 10^9$ for the hetero-nanospheres ($\text{Au}/\text{Al}_2\text{O}_3@\text{Ag}$) on the pyramidal structures. For SERS from metal nanoparticle, we note that both the SERS signal uniformity and the SERS enhancement factor remarkably surpass the previously reported values of SERS enhancement factor at the level of 10^6 and is also comparable to some recent results.^[30–33] Unlike random metallic nanosphere on the planar substrate, this type of pyramidal structure substrate can provide orderly functional design and high opportunities for reliable SERS application. Firstly, the pyramid-shaped structure has both projecting edges-corners and sharp apex, and then this Si pyramidal structure coated by double-layer Au nanosphere is similar to metallic pyramidal structure, which has a notable concentration and enhancement of electromagnetic field due to a geometry-induced enhancement at sharp apexes and projecting edges-corners, and can guide effectively surface plasmon polariton to concentrate at the apexes for improved SERS.^[34,35] On the other hand, this pyramid-shaped structure increases the specific surface area of the SERS substrate, enlarging the effective area of high-density hot spots to increase the number of probed molecules within a detection volume, compared to a planar SERS substrate.^[36–38] Therefore, it is clear that for optimized double-layer stacked $\text{Au}/\text{Al}_2\text{O}_3/\text{Au}(\text{Ag})$ nanospheres, some designed micro or nanostructure arrays can provide ideal functional platform to increase greatly their SERS properties and create more opportunities for practical applications.

3. Conclusion

This work presents a reproducible high-throughput nanofabrication technique to form large-area double-layers stacked

homo/hetero metal-nanospheres structures for highly intense SERS, which have very dense nanojunctions and sub-5 nm nanospacing with precise control by ultrathin alumina cladding of the metal nanospheres using ALD to generate high density SERS hot spots within a detection volume. This stacked metal nanospheres SERS substrate shows high average EF of over 10^7 and excellent uniformity and hence displays an increase of SERS signals by more than two orders of magnitude, compared to single-layer metal nanosphere substrate. Hetero-metal-nanospheres stacked structures (Ag–Au) was found to exhibit stronger electromagnetic coupling than homo-metal-nanosphere stacked structure (Au–Au) due to the combined effect of two resonances, and hence has a greater SERS EF. This method is not only applicable to form tunable nanospacing down to sub-5 nm with high-density nanojunction on the large-area 4 inch wafer, but can also be combined easily with other micro/nano-structure arrays, such as the pyramid-shaped structure arrays, which help very much to increase further the SERS signals with EF over 10^8 . Our results indicated double-layer stacked $\text{Au}/\text{Al}_2\text{O}_3@\text{Au}(\text{Ag})$ nanosphere structure is an ideal bio-analytical platform to combine SERS bio-sensing. Considering high SERS enhancement factor on one hand, and on the other hand, the reproducibility, the familiarity of the basic techniques, the wafer-scale and the widespread usage of the stacked $\text{Au}/\text{Al}_2\text{O}_3@\text{Au}(\text{Ag})$ nanosphere substrate, we believe that this simple and reliable method offers an effective way for enabling quantitative SERS and promoting practical application of this SERS substrate.

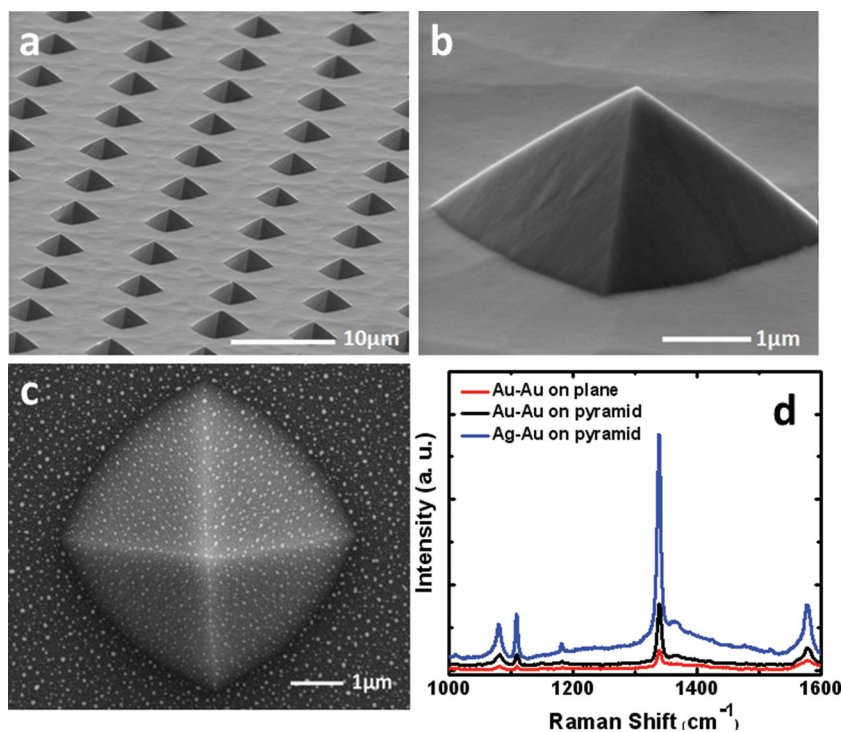


Figure 7. SEM images of a) pyramid-shaped silicon structure arrays without nanospheres and b) a single pyramid-shaped structure, also without nanospheres, and c) coated with double-layer stacked metal-nanospheres. d) SERS spectra of pyramid-shaped structures with different double-layer stacked metal-nanospheres structures.

4. Experimental Section

Fabrication of Layer-stacked Metal Nanospheres Structure: The fabrications of this plasmonic nanostructure need three kinds of processes: the metal film deposition, rapid thermal annealing (RTA), and atomic layer deposition (ALD). The Au nanofilms was deposited by electron beam evaporation (EBE) on the cleaned silicon substrates. A RTA technology was used to anneal the Au nanofilms under the temperature of 450 °C for 3 min, and consequently the surface morphology of Au nanofilm is changed from irregular nanoislands to nanospheres arrays. Different thickness Al₂O₃ films from 2 nm to 7 nm were deposited separately on the as-formed Au nanospheres by ALD under the temperature of 80 °C, and such lower growth temperature was chosen to avoid the impact on the lower-layer gold nanospheres.

Fabrication of Silicon Pyramid-shaped Structure Arrays Substrate: Four-step fabrication process are described as follow: First, the (100) silicon substrates were covered by 50 nm thick Si₃N₄ film using plasma-enhanced chemical vapor deposition. Second, the photo-resist of S1813 was spin-coated on the substrate and UV lithography process was carried out. Then the square arrays with a period of 9 μm and a side length of 5 μm are patterned on the substrate. In this step, we must make sure that the side direction of the squares parallel the silicon (100) plane. Third, the square pattern was transferred to Si₃N₄ film utilizing reactive ion etching with an etching duration of about 1 min. Finally, the KOH solution of 32% by weight was used to etch the samples under the temperature 80 °C for 3–4 min. So the pyramid-shaped structure was obtained, which is according to the fact that the ratio of silicon (100)/(111) etch rates vary from 20:1 to 200:1 reported in the literatures.^[39–41]

SERS Measurements: First, the reflectance spectra was firstly measured to make sure the plasmon resonance ω_p , using a home-made integrated microscope-spectrometer system. Second, the solution of 4-NBT with 100 μM was prepared, and also this solution concentrations can be diluted down to 10 nM for a quantitative analysis of SERS. Then about 0.05 mL solution was dropped and spread on the surface of the samples to keep for 4 h. After a final wash process, a monomolecular layer of 4-NBT can be self-assembled on the surface of gold spheres. Third, SERS measurements were completed with the excitation laser wavelength of 532 nm and the power of 0.65 mW. An objective lens is used to focus the excitation laser on the samples and collect the emitted Raman signals with 2 μm laser spot. For the SERS measurement of Si pyramidal substrates, all measurement-spots are randomly selected on a single Si pyramid structure with a tip and four planar sides.

Calculation SERS Enhancement Factor: The enhancement factor for the stacked Au nanosphere structure substrate was characterized using the intense stretching vibration mode from 4-NBT at 1340 cm⁻¹ Raman shift and widely used equation for the average SERS EF: $EF = (I_{SERS}/N_{Surf})/(I_{RS}/N_{Vol})$, where N_{Surf} is the average number of 4-NBT molecules contributing to the normal Raman scattering signal, N_{Vol} is the average number of 4-NBT molecules contributing to the SERS signal, and I_{SERS} and I_{bulk} are the intensities of the scattering band of interest for the SERS and normal Raman spectra, respectively.^[42,43] Considering a rigorous definition of N_{Surf} and N_{Vol} ,^[43] $N_{Surf} = \mu_M \mu_S A_M$ and $N_{Vol} = C_{RS} H_{eff}$, where μ_M is the surface density of the individual nanostructures producing the enhancement, and μ_S is the surface density of molecules on the

metal, A_M represents the surface metallic area of the individual nanostructures, C_{RS} is the concentration of the solution used for the non-SERS measurement, and H_{eff} is the effective height of the scattering volume. For stacked nanosphere plane structure substrate in this work, $\mu_M \approx 1.1 \times 10^{11}/\text{cm}^2$, $\mu_S \approx 1.2 \times 10^{15}/\text{cm}^2$, $A_M \approx 8 \times 10^{-12} \text{ cm}^2$, $C_{RS} = 1 \text{ mol/l}$, $H_{eff} = 20 \mu\text{m}$, but SERS detection is enhanced several times in the pyramidal structure due to increased surface area.

Acknowledgements

The authors acknowledge the National Natural Science Foundation of China (Grand No. 11174362, 91023041, 91323304, 51272278, 61390503), and the Knowledge Innovation Project of CAS (Grand No. KJCX2-EW-W02)

-
- [1] S. Gresillon, L. Aigouy, A. C. Boccara, J. C. Rivoal, X. Quelin, C. Desmarest, P. Gadenne, V. A. Shubin, A. K. Sarychev, V. M. Shalaev, *Phys. Rev. Lett.* **1999**, *82*, 4520.
 - [2] C. E. Talley, J. B. Jackson, C. Oubre, N. K. Grady, C. W. Hollars, S. M. Lane, T. R. Huser, P. Nordlander, N. J. Halas, *Nano Lett.* **2005**, *5*, 1569.
 - [3] S. Y. Lee, L. Hung, G. S. Lang, J. E. Cornett, I. D. Mayergoyz, O. Rabin, *ACS Nano* **2010**, *4*, 5763.
 - [4] J. S. Huang, J. Kern, P. Geisler, P. Weinmann, M. Kamp, A. Forchel, P. Biagioni, B. Hecht, *Nano Lett.* **2010**, *10*, 2105.
 - [5] A. Alu, N. Engheta, *Phys. Rev. Lett.* **2010**, *104*, 13902.
 - [6] D. C. Marinica, A. K. Kazansky, P. Nordlander, J. Aizpurua, A. G. Borisov, *Nano Lett.* **2012**, *12*, 133.
 - [7] J. F. Li, Y. F. Huang, Y. Ding, Z. L. Yang, S. B. Li, X. S. Zhou, F. R. Fan, W. Zhang, Z. Y. Zhou, D. Y. Wu, B. Ren, Z. L. Wang, Z. Q. Tian, *Nature* **2010**, *464*, 392.
 - [8] M. Ringler, A. Schwemer, M. Wunderlich, A. Nichtl, K. A. Kürzinger, T. Klar, J. Feldmann, *Phys. Rev. Lett.* **2008**, *100*, 203002.
 - [9] S. S. Acimovic, M. P. Kreuzer, M. U. González, R. Quidant, *ACS Nano* **2009**, *3*, 1231.
 - [10] K. Kneipp, Y. Wang, H. Kneipp, L. T. Perelman, I. Itzkan, R. Dasari, M. S. Feld, *Phys. Rev. Lett.* **1997**, *78*, 1667.
 - [11] S. Nie, S. R. Emory, *Science* **1997**, *275*, 1102.
 - [12] D. K. Lim, K. S. Jeon, H. M. Kim, J. M. Nam, Y. D. Suh, *Nat. Mater.* **2010**, *9*, 60.
 - [13] D. R. Ward, N. K. Grady, C. S. Levin, N. J. Halas, Y. P. Wu, P. Nordlander, D. Natelson, *Nano Lett.* **2007**, *7*, 1396.
 - [14] D. R. Ward, N. J. Halas, J. W. Cissék, J. M. Tour, Y. Wu, P. Nordlander, D. Natelson, *Nano Lett.* **2008**, *8*, 919.
 - [15] S. Sheikholeslami, Y. Jun, P. K. Jain, P. Alivisatos, *Nano Lett.* **2010**, *10*, 2655.
 - [16] E. R. Encina, E. A. Coronado, *J. Phys. Chem. C* **2011**, *115*, 15908.
 - [17] S. Hong, X. Li, *J. Nanomater.* **2013**, *2013*, 1.
 - [18] S. E. J. Bell, M. R. McCourt, *Phys. Chem. Chem. Phys.* **2009**, *11*, 7455.
 - [19] L. Khriachtchev, L. Heikkila, T. Kuusela, *Appl. Phys Lett.* **2001**, *78*, 1994.
 - [20] D. V. Voronine, A. M. Sinyukov, X. Hua, K. Wang, P. K. Jha, E. Munusamy, S. E. Wheeler, G. Welch, A. V. Sokolov, M. O. Scully, *Sci. Rep.* **2012**, *89*, 2.
 - [21] F. S. Ou, M. Hu, I. Naumov, A. Kim, W. Wu, A. M. Bratkovsky, X. Li, R. S. Williams, Z. Li, *Nano. Lett.* **2011**, *11*, 2538.
 - [22] A. Aubry, D. Y. Lei, S. A. Maier, J. B. Pendry, *ACS Nano* **2010**, *5*, 3293.

- [23] B. Dong, Y. Fang, L. Xia, H. Xu, M. Sun, *J. Raman Spectrosc.* **2011**, *42*, 1205.
- [24] C. Ciraci, R. T. Hill, J. J. Mock, Y. Urzhumov, A. I. Fernández-Domínguez, S. A. Maier, J. B. Pendry, A. Chilkoti, D. R. Smith, *Science* **2012**, *337*, 1072.
- [25] D. C. Marinica, A. K. Kazansky, P. Nordlander, J. Aizpurua, A. G. Borisov, *Nano Lett.* **2012**, *12*, 1333.
- [26] S. Lin, W. Zhu, Y. Jin, K. B. Crozier, *Nano Lett.* **2013**, *13*, 559.
- [27] A. Lombardi, M. P. Grzelczak, A. I. Crut, P. Maioli, I. Pastoriza-Santos, L. M. Liz-Marzan, N. D. Fatti, F. Vallee, *ACS Nano* **2013**, *7*, 2522.
- [28] S. Sheikholeslami, Y. Jun, P. K. Jain, P. Alivisatos, *Nano Lett.* **2010**, *10*, 2655.
- [29] G. Bachelier, I. Russier-Antoine, E. Benichou, C. Jonin, N. Del Fatti, F. Vallée, P.-F. Brevet, *Phys. Rev. Lett.* **2008**, *101*, 197401.
- [30] V. Liberman, C. Yilmaz, T. M. Bloomstein, S. Somu, Y. Echegoyen, A. Busnaina, S. G. Cann, K. E. Krohn, M. F. Marchant, M. Rothschild, *Adv. Mater.* **2010**, *22*, 4298.
- [31] M. J. Mulvihill, X. Y. Ling, J. Henzie, P. Yang, *J. Am. Chem. Soc.* **2010**, *132*, 268.
- [32] W. Lee, S. Y. Lee, R. M. Briber, O. Rabin, *Adv. Funct. Mater.* **2011**, *21*, 3424.
- [33] K. L. Wustholz, A. I. Henry, J. M. McMahon, R. G. Freeman, N. Valley, M. E. Piotti, M. J. Natan, G. C. Schatz, R. P. Van Duyne, *J. Am. Chem. Soc.* **2010**, *132*, 10903.
- [34] N. A. Issa, R. Guckenberger, *Opt. Exp.* **2007**, *15*, 12131.
- [35] J. M. Kontio, H. Husu, J. Simonen, M. J. Huttunen, J. Tommila, M. Pessa, M. Kauranen, *Opt. Lett.* **2009**, *34*, 1979.
- [36] Y. Oh, K. H. Jeong, *Adv. Mater.* **2012**, *24*, 2234.
- [37] M. S. Schmidt, J. Hübner, A. Boisen, *Adv. Mater.* **2011**, *24*, OP11.
- [38] S. Y. Baik, Y. J. Cho, Y. R. Lim, H. S. Im, D. M. Jang, Y. Myung, J. Park, H. S. Kang, *ACS Nano* **2012**, *6*, 2459.
- [39] K. Biswas, S. Kal, *Microelectron. J.* **2006**, *37*, 519.
- [40] A. Brockmeier, F. J. S. Rodriguez, M. Harrison, U. Hilleringmann, *J. Micromech. Microeng.* **2012**, *22*, 125012.
- [41] I. Zubel, K. Rola, *Opt. Appl.* **2011**, *41*, 423.
- [42] M. K. Hossain, Y. Kitahama, G. G. Huang, X. Han, Y. Ozaki, *Anal. Bioanal. Chem.* **2009**, *394*, 1747.
- [43] E. C. Le Ru, E. Blackie, M. Meyer, P. G. Etchegoin, *J. Phys. Chem. C* **2007**, *111*, 13794.

Received: February 24, 2014

Revised: June 10, 2014

Published online: July 3, 2014